

crystalline surface protein layer. *FEMS Microbiol. Lett.*, 1999, **179**, 275–280.

21. Selvakumar, R. *et al.*, As(V) removal using carbonized yeast cells containing silver nanoparticles. *Water Res.*, 2011, **45**, 583–592
22. Langmuir, I., The adsorption of gases on plane surfaces of glass, mica and platinum. *J. Am. Chem. Soc.*, 1918, **40**, 1361.
23. Aytas, S., Alkim Turkozu, D. and Gok, C., Biosorption of uranium (VI) by bi-functionalized low cost biocomposite adsorbent. *Desalination*, 2011, **280**, 354–362.
24. Shuibo, X., Chun, Z., Xinghuo, Z., Jing, Y., Xiaojian, Z. and Jingsong, W., Removal of uranium (VI) from aqueous solution by adsorption of hematite. *J. Environ. Radioact.*, 2009, **100**, 162.
25. Jung, Y., Kim, S., Park, S. J. and Kim, J. M., Application of polymer-modified nanoporous silica to adsorbents of uranyl ions. *Colloids Surf. A*, 2008, **33**, 162.
26. Han, R., Zou, W., Wang, Y. and Zhu, L., Removal of uranium(VI) from aqueous solutions by manganese oxide coated zeolite: discussion of adsorption isotherms and pH effect. *J. Environ. Radioact.*, 2007, **93**, 127.

ACKNOWLEDGEMENTS. We thank the Indira Gandhi Centre for Atomic Research (IGCAR), Kalpakkam for providing financial support. We also thank Dr Rani P. George, Corrosion Science and Technology Division; Dr B. Venkataraman, Dr Balasundhar, Radiological Safety and Environment Group, IGCAR; Dr T. Subba Rao, Water and Stream Chemistry Division, BARC Facilities, Kalpakkam; Uranium Corporation of India and PSG Management, Coimbatore for help rendered throughout the study.

Received 2 December 2013; revised accepted 1 May 2014

Geochemistry of pegmatites from South Delhi Fold Belt: a case study from Rajgarh, Ajmer district, Rajasthan

Kumar Batuk Joshi¹, Soumya Ray¹, Deepak Joshi¹ and Talat Ahmad^{1,2,*}

¹Department of Geology, University of Delhi, Delhi 110 007, India

²University of Kashmir, Srinagar 190 006, India

On the basis of geochemical studies, pegmatites emplaced in the Rajgarh Group of Delhi Supergroup in the South Delhi Fold Belt have been classified into three groups. They show a variety of rare earth element enrichment patterns, LREE/HREE values and Eu anomalies. The geochemical affinities of these pegmatites suggest their calc-alkaline nature, volcanic arc granite signature in tectonic discrimination diagrams (Nb vs Y and Rb vs Nb + Y) and a probable S-type parentage as inferred from their high A/CNK value,

peraluminous character, presence of high normative corundum and abundance of garnet and muscovite. These features have been related to subduction-related processes which might have generated the parent granitic melt forming these pegmatites.

Keywords: Geochemical studies, granitic melt, pegmatites, subduction.

THAT pegmatites result from magmatic differentiation of granitic systems^{1–7} is almost unanimously agreed upon by geologists and therefore referred to as ‘granitic pegmatites’, although pegmatitic textures can result in igneous rocks of all compositions⁸. Pegmatites are representative of late-stage residual fraction of silicic melt that accumulate in the granitic parent magma itself or intrude the surrounding rocks⁹. However, it is not always mandatory for the pegmatites to be in close spatial association with the parent granite^{6,10}. The volatile-rich, residual, pegmatitic melt seems to favour stability at lower temperatures at large distances from the parent plutonic source^{6,11}. The enrichment of rare elements (Be, Ta, Li, Sn, Bi, W, Mo, Cu) and volatiles in the late residual magma^{6,12} renders the granite, pegmatites and hydrothermal veins subsequently formed substantially mineralized, economically viable and sought after. However, it is to be borne in mind that these rare element enriched-granitic pegmatites constitute about less than 1% by volume of the pegmatite terrain they are a part of¹³ and that not all pegmatite bodies can be exploited for their mineral content. One of the most rudimentary principles underlying geochemistry is the enrichment of the compatible and incompatible elements in the fractionating minerals and residual melt respectively. These preferential behaviours and consequent chemical signatures have formed the basis of characterization and differentiation of one rock from the other and even give an account of their possible evolution and parentage. The accentuated trace element signatures that pegmatite inherit from their granitic sources can be used to fingerprint their origin¹³.

The NE–SW trending Aravalli–Delhi orogen which runs across Rajasthan separates the Marwar and Mewar cratons and comprises of the Aravalli Fold Belt and the Delhi Fold Belt¹⁴. The South (SDFB) and North Delhi Fold Belts form the principal divisions of the Proterozoic Delhi Fold Belt^{15–17} and expose rocks of the Delhi Supergroup¹⁴. The SDFB comprises of the western Sendra basin (consisting of the Barotiya and Sendra Group of rocks) and the eastern Bhim basin (consisting of the Rajgarh and Bhim Group of rocks)¹⁸ which are separated by an inlier of pre-Delhi rocks^{14,19}. Several hypotheses regarding the evolution of the Delhi Fold Belt have been put forward by previous workers. Heron²⁰ proposed that sedimentation took place in intracontinental fault-bound grabens. However, the more popular diachronous development model was proposed by Sinha-Roy^{15,16}, wherein

*For correspondence. (e-mail: tahmad001@yahoo.co.in)

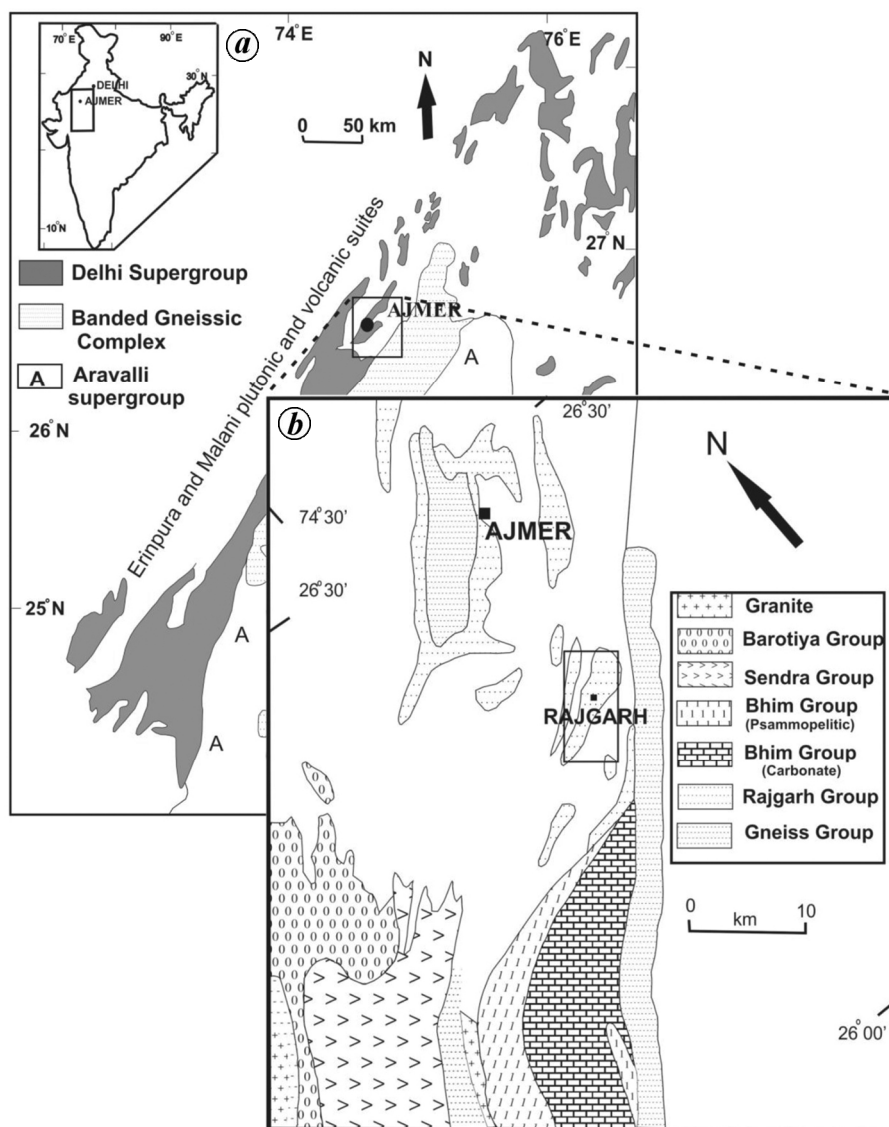


Figure 1. *a*, Geological map of the Delhi Fold Belt (adapted from Pandit *et al.*³¹ and references therein). *b*, Generalized geological map of the South Delhi Fold Belt showing the study area (adapted from Mukhopadhyay and Bhattacharyya³²).

the Delhi rift system was divided into the North Delhi Rift (NDR) and South Delhi Rift (SDR) by an intracontinental strike-slip fault (Sambhar–Jaipur–Dausa Fault). The failure of NDR and opening of the SDR into an oceanic basin resulted in the westwards subduction of the Delhi oceanic crust and consequent island arc formation in the west which manifested as the Sendra Group of the western basin of SDFB. The island arc nature of the rocks of the western part of SDFB have also been confirmed by Sugden and Windley²¹, and Deb and Sarkar²².

The present study is confined to SDFB and involves initial geochemical investigations of 14 pegmatite samples from Rajgarh, Ajmer district, Rajasthan (Figure 1). The studied pegmatites intrude garnetiferous mica schist and

schistose ultrabasic rocks (Figure 2) of the Delhi Supergroup of rocks²³ belonging to the Rajgarh Group exposed in the eastern Bhim basin of SDFB. The pegmatites are coarse grained, inequigranular and show typical pegmatitic texture. The commonly lensoidal pegmatite veins are composed predominantly of quartz and subordinate amounts of perthitic microcline, plagioclase and muscovite²³. This study aims at geochemically characterizing the pegmatites and makes an attempt to infer their genesis.

These pegmatic bodies are mostly unzoned. Petrographic studies reveal that these pegmatites consist principally of quartz, K-feldspar and plagioclase. Garnet, muscovite, tourmaline crystals and subordinate biotite and zircon are commonly present in them. Unzoned

Table 1. Major and trace element data of Rajgarh pegmatites

Elements	Group 1					Group 2					Group 3				
	D4S6	D4S10	D6S2/3	D6S5	D6S6	D6S10/1	D6S9	D6S9/1	D6S9/2	D6S1	D4S9	D6S2/4	D6S10/2	D6S8	
SiO ₂	66.9	72.85	72.65	74.88	70.01	73.55	74.88	71.22	68.22	69.99	74.88	75.88	75.28	73.55	
Al ₂ O ₃	22.06	16.88	15.22	14.8	20.65	15.98	15.66	19.59	20.55	18.91	15.66	15.66	17.88	15.98	
FeO	1.12	0.53	1.37	0.39	0.45	1.07	0.82	0.14	0.24	0.36	0.81	0.14	0.18	0.3	
Fe ₂ O ₃	0.47	0.22	0.56	0.16	0.18	0.44	0.33	0.06	0.1	0.15	0.34	0.06	0.08	0.13	
MnO	0.03	0.14	1.09	0.08	0.01	0.05	0.02	0.77	0.9	0.01	0.02	0.02	0.01	0.02	
MgO	0.16	0.05	0.04	0.01	0.21	0.08	0.1	0.01	0.02	0.04	0.1	0.02	0.03	1.12	
CaO	0.07	0.71	0.54	0.85	0.57	1	1.42	0.21	0.03	0.8	1.42	0.92	0.59	1.5	
Na ₂ O	1.23	6.34	5.41	4.93	1.66	4.15	4.67	1.76	1.81	7.61	4.67	5.34	3.25	5.18	
K ₂ O	5.82	0.17	1.63	2	4.62	1.93	0.65	5.03	6.55	0.64	0.65	0.07	1.59	0.92	
TiO ₂	0.09	0.01	0.02	0.01	0.02	0.02	0.03	0.02	0.03	0.02	0.03	0.01	0.03	0.02	
P ₂ O ₅	0.08	0.04	0.04	0.05	0.28	0.09	0.03	0.01	0.02	0.05	0.03	0.02	0.03	0.04	
LOI	0.77	0.51	0.38	0.87	0.54	0.79	0.74	0.81	0.67	0.57	0.95	0.95	0.33	0.86	
Sum	98.8	98.45	98.95	99.03	99.2	99.15	99.35	99.63	99.14	99.15	99.56	99.09	99.28	99.62	
V	8	3	4	2	2	4	3	1	3	2	4	5	3	7	
Cr	17	15	19	13	8	19	11	7	8	8	15	16	14	12	
Co	1	1	1	1	1	2	1	<1	1	2	2	1	1	3	
Ni	14	13	14	10	10	19	10	5	5	5	15	12	8	9	
Cu	1	2	1	1	1	3	3	1	2	2	3	1	2	1	
Zn	8	41	27	11	9	48	10	11	41	12	56	5	12	8	
Ga	36	14	18	16	20	12	25	28	42	21	12	14	15	13	
Rb	568	31	162	133	204	138	250	5001	7516	46	36	27	142	71	
Sr	5	17	11	13	28	39	9	6	16	12	29	14	26	17	
Y	8	8	59	15	15	34	<1	<1	<1	3	4	1	2	4	
Zr	32	50	209	52	41	88	13	20	4	34	27	15	13	17	
Nb	44	2	3	5	14	1	164	190	58	3	4	2	9	2	
Cs	24	2	5	8	9	22	104	2635	3797	1	2	1	24	4	
Ba	72	30	43	31	54	57	27	16	27	25	47	20	50	39	
Th	5	2	11	6	5	2	<1	2	bdl	bdl	2	1	1	1	
U	2	2	22	8	4	3	1	1	bdl	3	1	1	1	1	
La	12.51	1.85	7.43	7.59	10.68	17.85	0.44	0.49	0.47	0.86	2.33	2.48	2.29	2.23	
Ce	24.49	3.89	18.65	14.24	22.03	35.28	0.83	0.76	1.09	1.63	4.78	4.28	4.32	4.25	
Pr	2.45	0.42	2.05	1.52	2.22	3.92	0.09	0.08	0.14	0.19	0.48	0.40	0.45	0.45	
Nd	9.16	1.44	7.04	5.21	7.81	14.06	0.30	0.24	0.33	0.60	1.76	1.13	1.55	1.62	
Sm	1.81	0.52	3.24	1.61	1.86	3.33	0.06	0.05	0.09	0.18	0.44	0.30	0.32	0.36	
Eu	0.18	0.03	0.03	0.05	0.17	0.15	0.01	0.01	0.02	0.03	0.09	0.06	0.12	0.07	
Gd	1.35	0.42	3.74	1.26	1.48	2.86	0.05	0.04	0.05	0.19	0.38	0.18	0.27	0.38	
Dy	1.42	1.12	10.43	2.24	2.40	4.84	0.06	0.07	0.05	0.39	0.68	0.24	0.34	0.59	
Er	0.72	0.93	4.71	1.89	1.46	3.47	0.04	0.04	0.03	0.23	0.53	0.15	0.21	0.40	
Yb	0.54	1.17	2.70	2.39	1.39	3.90	0.05	0.03	0.04	0.22	0.64	0.15	0.20	0.42	
Lu	0.09	0.19	0.35	0.40	0.24	0.64	0.01	0.01	0.00	0.04	0.11	0.02	0.03	0.07	
Total ΣREE	54.70	11.96	60.37	38.41	51.73	90.32	1.93	1.82	2.31	4.54	12.22	9.41	10.11	10.83	
(La/Yb)N	16.52	1.13	1.98	2.28	5.53	3.28	6.98	10.38	8.55	2.85	2.60	11.72	8.07	3.83	
(Eu/Eu*)	0.33	0.16	0.02	0.11	0.31	0.14	0.62	0.68	0.82	0.52	0.66	0.7	1.25	0.61	

Major oxides are in wt% and trace elements in ppm. Bdl, Below detection limit.

nature of the pegmatites rendered sample collection somewhat easy. Representative fresh samples were collected and major element analyses were carried out using X-ray fluorescence spectrometry (Phillips MAGIX PRO model 2440) within 3% relative standard deviation²⁴. Trace elements were also determined at the National Geophysical Research Institute, Hyderabad using inductively coupled plasma mass spectrometer (Perkin Elmer ELAN DRC II) and precision better than 5% for majority of trace elements and up to 10% for few HREE was achieved²⁵. The geochemical data of the Rajgarh pegmatites are enlisted in Table 1.

The pegmatites from Rajgarh area are calc-alkaline with silica ranging from 66.9% to 75.88% (average 72.48%). Alumina being the second most abundant oxide ranges from 14.8% to 22.06% (average 17.53%). A highly peraluminous character is exhibited by the high A/CNK value (average 1.70), which is consistently greater than that for all samples and normative corundum ranges from 3.46% to 15.50%. The pegmatites show Σ REE content ranging from 1.82 to 90.32 ppm. Based on distinct patterns shown in chondrite normalized REE diagrams, we grouped these pegmatite samples into three groups (Figure 3). All the

groups are characterized by LREE enrichments and variable degrees of HREE depletion. Group 1 with the highest Σ REE content (avg 51.25 ppm), yields the most pronounced negative Eu-anomaly ($Eu/Eu^* = 0.18$) and weak depletion of the HREE ($La_N/Yb_N = 5.12$). Group 2 has the lowest Σ REE content (avg. 2.02 ppm) and shows slight to no negative Eu anomaly ($Eu/Eu^* = 0.71$) and highest HREE depletion ($La_N/Yb_N = 8.64$). Group 3 has Σ REE

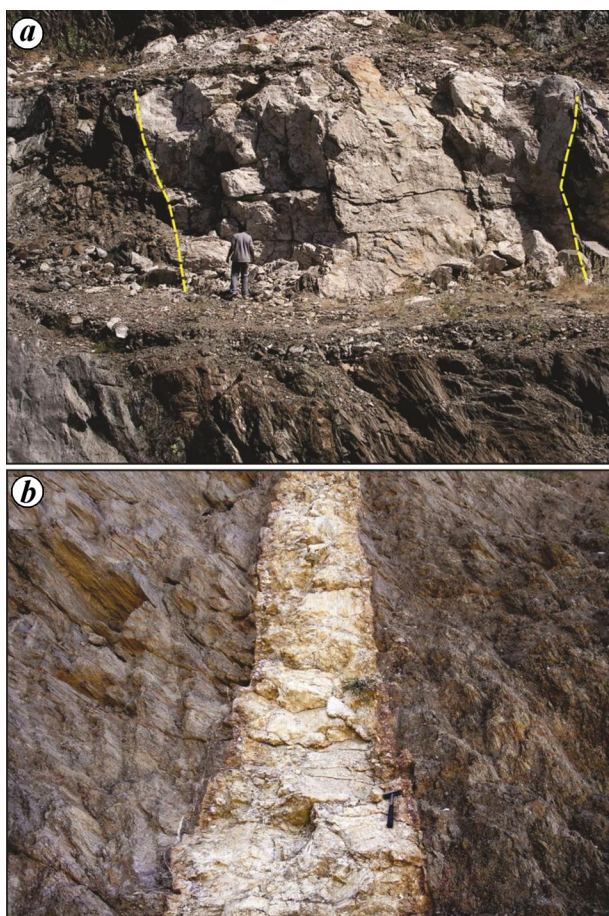


Figure 2 a, b. Pegmatite intruding host rocks of Delhi Supergroup.

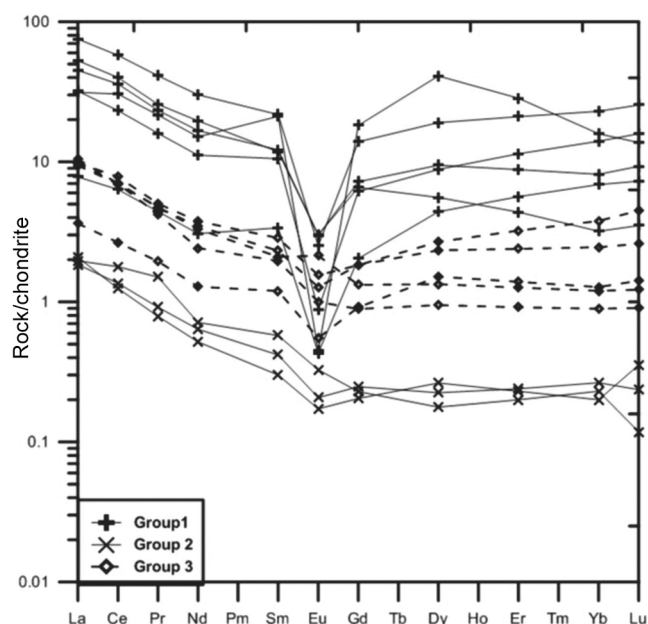


Figure 3. Chondrite normalized REE patterns for Rajgarh pegmatites. Chondrite elemental values taken from Sun and McDonough³³.

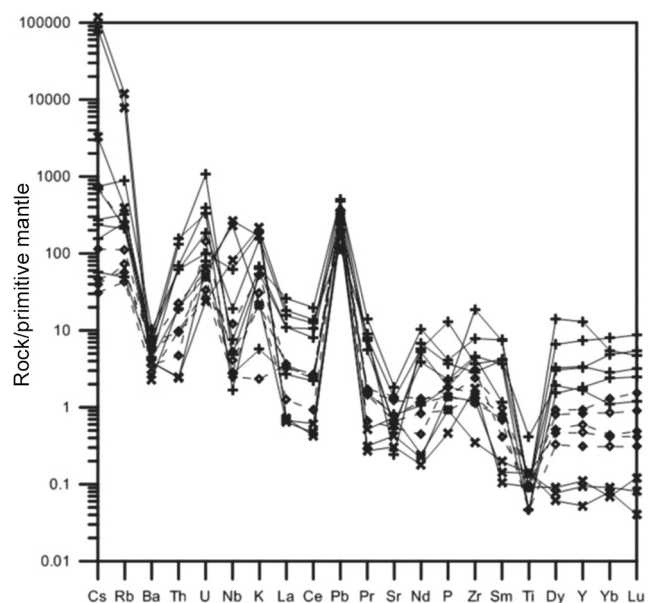


Figure 4. Primitive mantle normalized multi element diagrams for Rajgarh pegmatites. Primitive mantle elemental values taken from Sun and McDonough³³.

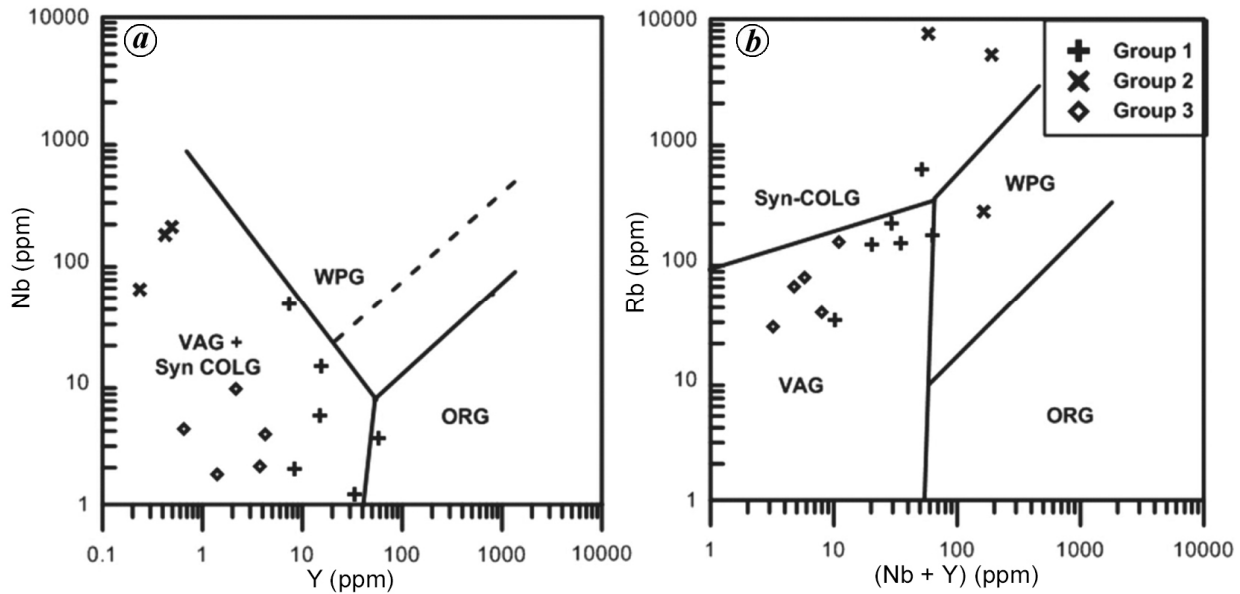


Figure 5. Nb versus Y (a) and Rb versus (Nb + Y) (b) tectonic discrimination diagrams of Pearce *et al.*³⁴. VAG, Volcanic arc granites; Syn, COLG, Collisional granites; WPG, Within plate granites; ORG, Ocean ridge granites. The x-axis has been modified to accommodate low values of Y in the samples.

content (avg 9.42 ppm) intermediate between groups 1 and 2 and exhibits relatively flatter REE patterns with moderate negative to positive Eu anomaly and HREE depletion ($La_N/Yb_N = 5.81$).

Peraluminous nature, high normative corundum (>1%), and abundant garnet and muscovite content may indicate S-type granitic parentage^{26,27} and consequent categorization of these pegmatites into LCT (enriched in lithium, caesium and tantalum) subtype^{1,13,28}. The low to moderate LREE/HREE value can be attributed to the crystallization of garnet which incorporates HREE into its crystal structure, thereby impeding HREE depletion. This is corroborated by the presence of abundant garnet crystals in the pegmatitic bodies. According to Hanson²⁹, the fractionation of garnet leads to depletion of HREE and a positive Eu anomaly in the melt. The relatively high HREE depletion and absence of conspicuous negative Eu anomaly exhibited by group 2 could point towards their crystallization from a late-stage melt in which the major portion of garnet crystals had already fractionated out. The low concentrations of Zr (44 ppm; <0.1%) possibly would not affect the HREE pattern during zircon crystallization²⁹ as opposed to the role played by garnet fractionation. The primitive mantle normalized multi-element diagrams for each of the groups are shown in Figure 4. The alkali metals (*viz.* Cs, Rb, K which also happen to be more mobile LIL elements) show enrichment, whereas the alkaline earth metals (Sr, Ba which are also LIL elements) show depletion indicating a highly differentiated parent pluton³⁰. The high concentrations of K and Rb could also be due to the abundance of muscovite and K-feldspar as Rb substitutes for K in these min-

erals. Fractionation of plagioclase and Ti-oxide manifests as Sr and Ti depletion respectively, because these mineral phases have high K_{DS} for these elements. However, group 2 pegmatites shows slight positive Sr anomaly, which along with the absence of conspicuous Eu anomaly can be correlated with localized plagioclase accumulation. It is interesting to note that the less mobile HFS elements (U, Th, Zr, Pb) also show enrichment which is the typical crustal signature. The pegmatitic melt owes its incompatible element (both HFSEs and LILEs) enrichment to its late-stage residual nature. When plotted in trace element (Nb vs Y, and Rb vs Y + Nb) discriminant diagrams (Figure 5), clear majority of the samples plot in the syn-collisional (syn COLG)–volcanic arc granites (VAG) field.

The inferred peraluminous, S-type granitic parent coupled with calc-alkaline nature and syncollisional + VAG signatures of these pegmatites indicate that the parent granitic melt and consequent pegmatitic bodies could be related to subduction processes. As discussed earlier, island arc formation in the west sector of SDFB has been reported by Sinha-Roy^{15,16}. One possible parent source could be the granitoids occurring in the western Sendra-Barotiya basin. However, due to paucity of data, geochemical comparisons between these granites and the pegmatites from Rajgarh have not been carried out.

In this study, we have geochemically characterized the Rajgarh pegmatites and tried to infer their parentage. Whether these pegmatites are genetically related to the granites exposed in the western basin remains unanswered and could be addressed in future studies. The spatial separation between the two basins should not be a

deterrent as pegmatites are known to form at large distances from their parent granitic melt^{6,10,11}. Elaborate studies on these pegmatites and their relationship with co-existing rocks would provide further insight into their genesis and emplacement.

1. Černý, P., Geochemical and petrogenetic features of mineralization in rare-element granitic pegmatites in the light of current research. *Appl. Geochem.*, 1992, **7**, 393–426.
2. Leal Gomes, C., Paragenetic analysis of state transition and paroxysmal evolution in granitic pegmatite systems of Central-Iberian Pegmatite Belt – structural, mineralogical and geochemical data. In Proceedings of the VII National Geological Congress (eds Mirão, J. and Balbino, A.), Estremoz, Portugal, 2006, pp. 1169–1175.
3. Neiva, A. M. R., Gomes, M. E. P., Ramos, J. M. F. and Silva, P. B., Geochemistry of granitic aplite–pegmatite sills and their minerals from Arcozelo da Serra area (Gouveia, Central Portugal). *Eur. J. Mineral.*, 2008, **20**, 465–485.
4. Neiva, A. M. R., Silva, P. B. and Ramos, J. M. F., Geochemistry of granitic aplite–pegmatite veins and sills and their minerals from the Sabugal area, central Portugal. *Neues Jahrb. Mineral., Abh.*, 2012, **189**(1), 49–74.
5. Neiva, A. M. R. and Ramos, J. M. F., Geochemistry of granitic aplite–pegmatite sills and petrogenetic links with granites, Guarda–Belmonte area, central Portugal. *Eur. J. Mineral.*, 2010, **22**, 837–854.
6. Antunes, I. M. H. R., Neiva, A. M. R., Ramos, J. M. F., Silva, P. B., Silva, M. M. V. G. and Corfu, F., Petrogenetic links between lepidolite-subtype aplite–pegmatite, aplite veins and associated granites at Segura (central Portugal). *Chem. Erde – Geochem.*, 2013 (in press).
7. Zhu, Y. F., Zeng, Y. and Gu, L., Geochemistry of the rare metal-bearing pegmatite no. 3 vein and related granites in the Keketuohai region, Altay Mountains, northwest China. *J. Asian Sci.*, 2005, **27**, 61–77.
8. London, D. and Kontak, D. J., Granitic pegmatites: scientific wonders and economic bonanzas. *Elements*, 2012, **8**, 257–261.
9. London, D., Granitic pegmatites: an assessment of current concepts and directions for the future. *Lithos*, 2005, **80**, 281–303.
10. Currie, K. L., Whalen, J. B., Davis, W. J., Longstaffe, F. J. and Cousens, B. L., Geochemical evolution of peraluminous plutons in southern Nova Scotia, Canada – a pegmatite-poor suite. *Lithos*, 1998, **44**, 117–140.
11. Černý, P., Massau, M., Goad, B. E. and Ferreira, K., The Greer Lake leucogranite, Manitoba, and the origin of lepidolite-subtype granitic pegmatites. *Lithos*, 2005, **80**, 305–321.
12. Beurlen, H., Marcelo, R. R. S. and Castro, C., Fluid inclusions in Be–Ta (Li–Sn)-bearing pegmatites from the Borborema Province, Northeast Brazil. *Chem. Geol.*, 2001, **173**, 107–123.
13. Černý, P., London, D. and Novák, M., Granitic pegmatites as reflections of their sources. *Elements*, 2012, **8**, 289–294.
14. Ramakrishnan, M. and Vaidyanathan, R., *Geology of India*, Geological Society of India, Bangalore, 2008, vol. 1, p. 556.
15. Sinha-Roy, S., Precambrian crustal interaction in Rajasthan, NW India. *Indian J. Earth Sci.*, 1984, 84–91.
16. Sinha-Roy, S., Proterozoic Wilson cycles in Rajasthan. *Mem. Geol. Soc. India*, 1988, **7**, 95–107.
17. Sinha-Roy, S., Malhotra, G. and Mohanty, M., *Geology of Rajasthan*, Geological Society of India, Bangalore, 1998, p. 278.
18. Gupta, P., Fareeduddin, Reddy, M. S. and Mukhopadhyay, K., Stratigraphy and structure of Delhi Supergroup of rocks in central part of Aravalli Range. *Rec., Geol. Surv. India*, 1995, **120**(2–8), 12–26.
19. Roy, A. B. and Jakhar, S. R., *Geology of Rajasthan, Northwest India: Precambrian to Recent*, Scientific Publishers (India), Jodhpur, 2002, p. 421.
20. Heron, A. M., The geology of Central Rajputana. *Mem. Geol. Surv. India*, 1953, **79**, p. 389.
21. Sugden, T. J. and Windley, B. F., Geotectonic framework of the early-mid Proterozoic Aravalli–Delhi orogenic belt, N.W. India. *Geol. Assoc. Canada, Program with Abstracts*, 1984, vol. 9, p. 109.
22. Deb, M. and Sarkar, S. C., Proterozoic tectonic evolution and metallogenesis in the Aravalli–Delhi orogenic complex, northwestern India. *Precambrian Res.*, 1990, **46**, 115–137.
23. Datta, A. K., Geological milieu of Emeralds in the Rajgarh area, Ajmer district, Rajasthan. *Geol. Soc. India Bull.*, 1966, **3**, 29–33.
24. Krishna, A. K., Murthy, N. N. and Govil, P. K., Multielement analysis of soils by wavelength-dispersive X-ray fluorescence spectrometry. *At. Spectrosc.*, 2007, **28**, 202–214.
25. Balaram, V. and Rao, T. G., Rapid determination of REEs and other trace elements in geological samples by microwave acid digestion and ICP-MS. *At. Spectrosc.*, 2004, **24**, 206–212.
26. Chappell, B. W. and White, A. J. R., Two contrasting granite types. *Pac. Geol.*, 1974, **8**, 173–174.
27. Chappell, B. W. and White, A. J. R., Two contrasting granite types: 25 years later. *Aust. J. Earth Sci.*, 2001, **48**, 489–499.
28. Černý, P. and Ercit, T. S., The classification of granitic pegmatites revisited. *Can. Mineral.*, 2005, **43**, 2005–2026.
29. Hanson, G. N., Rare earth elements in petrogenetic studies of igneous systems. *Annu. Rev. Earth Planet. Sci.*, 1980, **8**, 371–406.
30. Luecke, W., Lithium pegmatites in the Leinster Granite (Southeast Ireland). *Chem. Geol.*, 1981, **34**, 195–233.
31. Pandit, M. K., Carter, L. M., Ashwal, L. D., Tucker, R. D., Torsvik, T. H., Jamtveit, B. and Bhushan, S. K., Age, petrogenesis and significance of 1 Ga granitoids and related rocks from the Sendra area, Aravalli Craton, NW India. *J. Asian Earth Sci.*, 2003, **22**, 363–381.
32. Mukhopadhyay, D. and Bhattacharyya, T., Tectono-stratigraphic framework of the South Delhi Fold Belt in the Ajmer–Beawer region, Central Rajasthan, India: a critical review. In *Crustal Evolution and Metallogeny in the Northwestern Indian Shield* (ed. Deb, M.), Narosa, New Delhi, 2000, pp. 126–137.
33. Sun, S. S. and McDonough, W. F., Chemical and isotopic systematics of oceanic basalts: implications for mantle composition and processes. *Geol. Soc. London, Spec. Publ.*, 1989, **42**, 313–345.
34. Pearce, J. A., Harris, N. B. W. and Tindle, A. G., Trace element discrimination diagrams for the tectonic interpretation of granitic rocks. *J. Petrol.*, 1984, **25**, 956–998.

ACKNOWLEDGEMENTS. We thank the Head, Department of Geology, University of Delhi for providing the necessary facilities and the anonymous reviewer for useful comments. We also thank the scientists of the XRF and ICP-MS Laboratory, NGRI, Hyderabad for analysing the samples. Critical comments from J. Elis Hoffmann have helped improve the manuscript. This is a contribution to IGCP-SIDA project number 599.

Received 27 December 2013; revised accepted 22 April 2014